Kinetic Control of Reactions of Electrogenerated Co(I) Macrocycles with Alkyl Bromides in a Bicontinuous Microemulsion

De-Ling Zhou, Jianxin Gao, and James F. Rusling*

Contribution from the Department of Chemistry, Box U-60, University of Connecticut, Storrs, Connecticut 06269-3060

Received October 4, 1994[⊗]

Abstract: Bicontinuous microemulsions made from dodecane, water, and didodecyldimethylammonium bromide (DDAB) were investigated as media for the catalytic reduction of *trans*-1,2-dibromocyclohexane and for S_N2 reactions of *n*-alkyl bromides with electrochemically generated Co(I) complexes. Macrocyclic complexes vitamin B_{12} (a cobalt corrin) and Co(salen) resided in the water phase, while the alkyl bromides resided in the oil phase of the microemulsion. Rates of these bimolecular reactions were comparable in bicontinuous microemulsions to those in homogeneous solvents. Rates of DBCH reduction 40-fold larger in the bicontinuous fluid than in a water-in-oil microemulsion may be caused by a larger interfacial area of the bicontinuous system. For a given alkyl halide, a linear relation between log k_1 and $E^{\circ\prime}_{Co(II)/Co(I)}$ was found for both catalytic and S_N2 reactions for rate constants in DMF and the microemulsion. Thus, kinetic differences are controlled by activation free energies governed mainly by the formal potential of the Co(II)/Co(I) redox couple, rather than by distribution of reactants between phases. Formal potentials in the microemulsion depended on specific interactions, such as those of $[Co^I(salen)]^-$ with cationic surfactant head groups or the influence of water phase pH on vitamin B_{12}.

Microemulsions are clear, stable mixtures of surfactant, oil, and water that may provide less toxic and less expensive replacements for organic solvents in a variety of applications.[1−4] Recent studies suggest that these microheterogeneous fluids can be used to control and enhance rates of electrochemical catalysis.[2−5] For example, better catalytic efficiencies were achieved in a bicontinuous microemulsion compared to homogeneous solvent for reductions of nonpolar organohalides but not for the polar trichloroacetic acid.[6] Enhanced rates were attributed to preconcentration of nonpolar reactants in a coadsorbed layer of surfactant and catalyst on the electrode. Such surface preconcentration can also improve catalytic rates at electrodes in micellar solutions.[2,3]

In contrast to the above situation in which bimolecular reactions occur on an electrode surface, reductions catalyzed by electrochemically generating vitamin B_{12s} [$B_{i2}Co(I)$] in a water-in-oil microemulsion had rates several orders of magnitude smaller than in homogeneous acetonitrile−water.[7] Decreased rates in this microemulsion were attributed to the physical separation of vitamin B_{12} which resided in water droplets and the nonpolar vicinal dibromides in the continuous oil phase.

Water-in-oil microemulsions are nonconductive and not easily adaptable to electrochemical synthesis, although electropolymerization in such media was achieved with special electrodes.[8] Oil-in-water microemulsions often have smaller oil phase volume fractions than w/o or bicontinuous systems,[4,5] which may limit their capacity to dissolve nonpolar reactants. Bicontinuous microemulsions feature an intimately mixed, dynamic, microheterogeneous network of oil and water with surfactant at the interface.[9] Bicontinuous fluids can be prepared with double-chain alkylammonium surfactants for a range of oil phase volume fractions from 0.4 to 0.99,[9,11] and can be tailored for specific applications. Solubilities for polar and nonpolar reactants are excellent.

Electrochemical reactions in bicontinuous microemulsions of didodecyldimethylammonium bromide, water, and oil were shown to be similar to a homogeneous organic solvent containing a proton donor.[10,11] These microemulsions are conductive by virtue of the ionic surfactant, and are directly usable for electrochemical synthesis. The microemulsion featured in the present work, for example, was used successfully for electrolytic dechlorination of halogenated biphenyls to hydrocarbons using polar and nonpolar catalysts.[12]

Intimate mixing of phases in bicontinuous microemulsions[9c] might facilitate kinetics of homogeneous bimolecular reactions with reactants in different phases. To test this idea, we compared the rates of several synthetically useful reactions initiated by electrogenerated cobalt(I) complexes in a bicontinuous microemulsion and homogenous *N,N*-dimethylformamide (DMF).

Specifically, we set out to examine catalytic reactions of Co(I) forms of Co(salen) (A), cobalt phthalocyaninetetrasul-

[⊗] Abstract published in *Advance ACS Abstracts,* January 1, 1995.

(1) Friberg, S. *Adv. Colloid Interface Sci.* **1990**, *32*, 167−182.

(2) Rusling, J. F. *Acc. Chem. Res.* **1991**, *24*, 75−81.

(3) Rusling, J. F. In *Electroanalytical Chemistry*; Bard, A. J., Ed.; Marcel Dekker: New York, 1994; Vol. 18, pp 1−88.

(4) Rusling, J. F. In *Modern Aspects of Electrochemistry;* Conway, B. E., Bockris, J. O'M., Eds.; Plenum Press: New York, 1994; No. 26, pp 49−104.

(5) Mackay, R. A. *Colloids Surf.* **1994**, *82*, 1−23.

(6) Kamau, G. N.; Hu, N.; Rusling, J. F. *Langmuir* **1992**, *8*, 1042−1044.

(7) Owlia, A.; Wang, Z.; Rusling, J. F. *J. Am. Chem. Soc.* **1989**, *111*, 5091−5098.

(8) Garcia, E.; Oppenheimer, L. E.; Texter, J. in *Electrochemistry in Colloids and Dispersions*, Mackay, R. A., Texter, J., Eds.; VCH Publishers: New York, 1992; pp 257−272.

(9) (a) Evans, D. F.; Mitchell, D. J.; Ninham, B. W. *J. Phys. Chem.* **1986**, *90*, 2817−2825. (b) Blum, F. D.; Pickup, S.; Ninham, B. W.; Chen, S. J.; Evans, D. F. *J. Phys. Chem.* **1985**, *89*, 711−713. (c) Chen, S. J.; Evans, D. F. Ninham, B.; Mitchell, D. J.; Blum, F. D.; Pickup, S. *J. Phys. Chem.* **1986**, *90*, 842−847.

(10) Iwunze, M. O.; Sucheta, A.; Rusling, J. F. *Anal. Chem.* **1990**, *62*, 644−649.

(11) Iwunze, M. O.; Rusling, J. F. *J. Electroanal. Chem.* **1991**, *303*, 267−270.

(12) Zhang, S.; Rusling, J. F. *Environ. Sci. Technol.* **1993**, *27*, 1375−1380.

0002-7863/95/1517-1127$09.00/0

Chart 1. Chemical Structures of (**A**) Co^{II}(salen), (**B**) $Co^{II}TSPcNa_4$, and (**C**) vitamin B_{12r}.

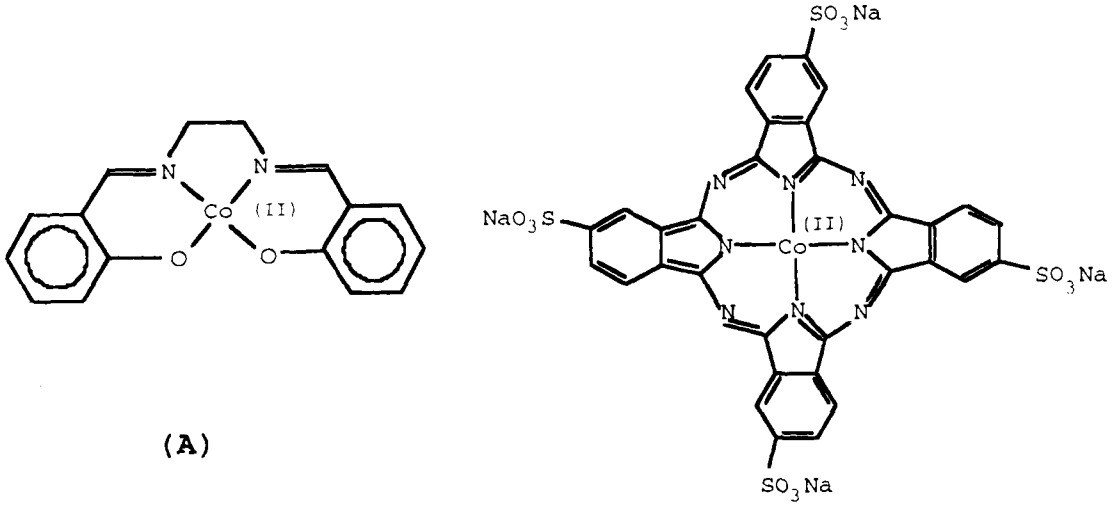

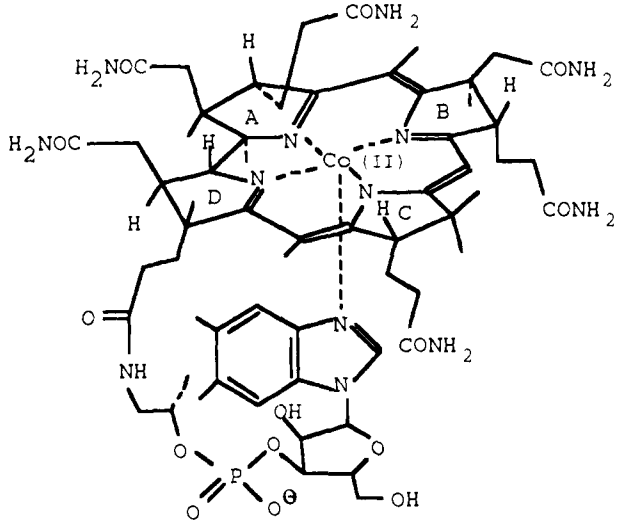

fonate (**B**), and vitamin B_{12} (**C**) with *trans*-1,2-dibromocyclohexane as well as S_N2 reactions of these complexes with *n*-alkyl bromides. These types of reactions are useful in a variety of electrosynthetic procedures.[13-18] Catalytic reduction of the vicinal dibromides yields olefins.[18] Reactions of the Co(I) complexes with alkyl halides yield relatively stable alkyl–cobalt complexes which can be used in subsequent carbon–carbon bond formation.[13-17]

Herein we show that rate constants comparable or faster than those in homogeneous solvent can be achieved in a bicontinuous microemulsion, as illustrated via bimolecular reactions of Co(I) complexes. Differences in rates for a given alkyl bromide depended mainly on the influence of the medium on the activation driving force for the reactions as governed by formal potentials of the Co(II)/Co(I) redox couples.

Experimental Section

Chemicals and Solutions. Vitamin B_{12a}, hydroxocob(III)alamin hydrochloride (99%), was from Sigma Co. Co(salen), N,N′-bis-(salicylidene)ethylenediaminocobalt(II), was synthesized according to a published procedure and purified by differential recrystallization.[19a,b] Tetrasodium salt of cobalt(II) 4,4′,4″,4‴-tetrasulfophthalocyanine 2-hydrate ($CoTSPcNa_4$) was prepared by a published method.[19c-e]

N,N-Dimethylformamide (DMF) was "Baker Analyzed" grade and treated with 4A molecular sieves overnight followed by vacuum distillation through a *Vigreux* column. Distilled water was purified with a Barnstead Nanopure system to a specific resistance >15 MΩ cm. Didodecyldimethylammonium bromide (DDAB, 99+%) and *n*-dodecane were from Eastman Kodak. *n*-Dodecyl bromide (97%) and (±)-*trans*-1,2-dibromocyclohexane (DBCH, 99%) were from Aldrich. *n*-Butyl bromide (BuBr) was from Aldrich and was distilled through a

(13) (a) Scheffold, R. In *Modern Synthetic Methods, Vol. 3*; Scheffold, R., Ed.; Wiley: New York, 1983; pp 355–439. (b) Iqbal, J.; Bhatia, B.; Nayyar, N. K. *Chem. Rev.* **1994**, *94*, 519–564.

(14) Scheffold, R.; Abrecht, S.; Orlinski, R.; Ruf, H.-R.; Stamouli, P.; Tinembart, O.; Walder, L.; Weymuth, C. *Pure Appl. Chem.* **1987**, *59*, 363–372.

(15) Scheffold, R. *Chimia* **1985**, *39*, 203–211.

(16) Torii, S. *Synthesis* **1986**, 873–886.

(17) (a) Busato, S.; Tinembart, O.; Zhang, Z.; Scheffold, R. *Tetrahedron* **1990**, *46*, 3155–3166. (b) Essig, S.; Scheffold, R. *Chimia* **1991**, *45*, 30–32.

(18) Connors, T. F.; Arena, J. V.; Rusling, J. F. *J. Phys. Chem.* **1988**, *92*, 2810–2816.

Vigreux column. Tetrabutylammonium bromide (TBABr) was from Eastman Kodak, twice recrystallized from ethyl acetate, and then dried in *vacuo*. All other chemicals were ACS reagent grade.

The bicontinuous microemulsion (DDAB:H_2O:dodecane; 21:39:40 wt%) was prepared by titrating the appropriate mixture of oil and DDAB with water as described previously.[10] Specific conductance was about 10^{-3} Ω^{-1} cm^{-1}. Solutions of cobalt complexes were prepared immediately before use.

Instrumentation and Methods. For cyclic voltammetry (CV), an EG&G PAR 273 electrochemical analyzer was used with Model 270/250 Software. Ohmic drop of the cell was compensated by this system. A gas-tight three-electrode, water jacketed cell was used. Temperature was 25 ± 1 °C. The working electrode was a glassy carbon disk with an active area of 0.072 cm^2 which was carefully polished with 0.05 μm alumina (Union Carbide) before each use. The reference was an aqueous saturated calomel electrode (SCE) separated from the solution by a salt bridge ending in porous Vycor. All potentials are referred to the SCE. The counter electrode was a platinum wire. Purified nitrogen was used to purge and blanket solutions to eliminate oxygen. For experiments with vitamin B_{12a}, the electrode was held *ca.* 15 s at −0.3 V before the potential scan was begun to assure a solution of vitamin B_{12r} [Co(II) form] near the electrode.[18] Oxygen-free alkyl bromide was introduced to the cell by a syringe through a silicon rubber septum. CVs were done under dimmed-light conditions to avoid photocleavage of in-*situ* generated alkyl−cobalt complexes.

UV−vis spectra were recorded by using a Perkin-Elmer λ6D spectrophotometer.

Rate Constants from Cyclic Voltammetry. Rate constants were estimated from the changes of CVs of the Co(II)/Co(I) redox couple. The ratio γ = [alkyl bromide]/[Co complex] and the scan rate were varied over appropriate ranges. Digital simulations were used to obtain theoretical curves of an experimental current ratio vs a kinetic parameter. Specific details are given in the Results section.

For the catalytic reductions, the solution electron transfer approximation was used in the simulation to account for the second electron transfer.[19f] For rate constants of alkylations, the ratio of the anodic peak in the presence (i_{pa}) of alkyl bromide to its value in the absence of alkyl bromide ($i_{pa}°$), $i_{pa}/i_{pa}°$, was used.[19g-j]

The program Digisim 1.0 (Bioanalytical Systems) was used for CV simulations.[19j] Parameters used are summarized in Table 1. The diffusion coefficients of DBCH as measured by CV were 2.0×10^{-5} cm^2 s^{-1} in 0.1 M TBABr/DMF and 1.1×10^{-5} cm^2 s^{-1} in the microemulsion. Reductions of *n*-BuBr and *n*-$C_{12}H_{25}Br$ could not be observed in the available potential window in 0.1 M TBABr/DMF or in the microemulsion. Thus, the diffusion coefficients of *n*-BuBr were taken to be the same as DBCH. For *n*-$C_{12}H_{25}Br$, the self-diffusion coefficient of dodecane[9b] in a similar microemulsion has been used (5.8×10^{-6} cm^2 s^{-1}). The diffusion coefficient of *n*-$C_{12}H_{25}Br$ in 0.1 M TBABr/DMF was estimated at 1.055×10^{-5} cm^2 s^{-1} by using Walden's rule.[20a]

Results

Electrochemistry of Co(II)/Co(I) Couples. The bicontinuous DDAB/water/dodecane (21/39/40) microemulsion chosen for this work has been characterized by a variety of methods,[9,10,21] including conductivity, viscosity, diffusivity, and small angle X-ray scattering. These studies showed that this fluid is continuous in both oil and water.

Table 1. Electrochemical Parameters of Co(II)/Co(I) Redox Couples[a]

complex	medium	$-E^{o\prime}$, V vs SCE	10^6D, cm^2 s^{-1}	$10^3k^{o\prime}$, cm s^{-1}
Co(salen)	DMF	1.225	5.2	8.2
	H_2O (pH 6)	1.26		
	DDAB μE[b]	1.085	0.55	4.5
vitamin B_{12}	DMF	0.710	1.8	3.0
	H_2O (pH 6)[c]	0.92		
	DDAB μE[b]	0.815	0.28	1.2
	H_2O/MeCN (pH 2.3)[c]	0.76	2.8	20
	AOT w/o μE[b,c]	0.80	0.63	6
CoTSPc	DMF	0.324	1.5	2
	DDAB μE[b]	0.250	d	d

[a]At glassy carbon working electrode; at 25 ± 1 °C; composition of microemulsion: DDAB/H_2O/dodecane = 21/39/40 (wt %). [b]Abbreviation of microemulsion. [c]Data from ref 7. [d]Not estimated owing to adsorption of the reactant on electrode.

We first investigated the cyclic voltammetry (CV) of the Co(II)/Co(I) redox couples of Co(salen) (**A**), cobalt phthalocyanine tetrasulfonate (**B**), and vitamin B_{12}r (**C**) in the microemulsion and in DMF. All complexes gave diffusion-controlled, reversible CVs at relatively low scan rates in the two fluid media, except for cobalt phthalocyanine tetrasulfonate (CoTSPc) in the microemulsion (Figure 1). In agreement with theory for diffusion controlled reactions,[20] peak currents for Co(salen) and vitamin B_{12} were proportional to square root of scan rate up to 1 V s^{-1}. Anodic and cathodic peak heights were equal, with about 60 mV separations which increased above 1 V s^{-1}. On the other hand, CoTSPc gave a peak current in the microemulsion that was directly proportional to scan rate, suggesting strong adsorption of this reactant onto the glassy carbon electrode.[20a]

Diffusion coefficients (D), apparent standard heterogeneous rate constants for electron transfer ($k^{o\prime}$), and formal potentials ($E^{o\prime}$) for the Co(II)/Co(I) redox couples were estimated from CV data by using standard procedures.[20] Diffusion coefficients (Table 1) decreased 6−9-fold in going from DMF to the microemulsion. Values are consistent with those found previously for water soluble ions in the DDAB microemulsion such as ferrocyanide (1×10^{-6} cm^2 s^{-1}) and ruthenium hexaammine (0.68×10^{-6} cm^2 s^{-1}).[10] The self-diffusion coefficient of water in these microemulsions is about 5-fold smaller than in bulk water,[9b] and DMF has a viscosity (0.92 cp)[22a] only slightly smaller than that of water (1 cp). Thus, the smaller diffusion coefficients for vitamin B_{12} and Co(salen) compared to DMF are consistent with residence of these complexes in the water phase of the microemulsion. Much larger D values are expected for solutes residing in the oil phase.[10]

Electron transfer rate constants ($k^{o\prime}$) for Co(II)/Co(I) couples were about 2−3-fold smaller in the microemulsion than in DMF. This was observed previously for metal complexes in DDAB microemulsions[10] and may be related to adsorbed surfactant on the electrode.[3]

Formal potentials (Table 1), as indicated by midpoints between anodic and cathodic peaks (Figure 1), were more positive for Co(salen) and CoTSPc in the microemulsion compared to DMF. Enough reversibility in square wave

(19) (a) Gilbert, W. C.; Taylor, L. T.; Dillard, J. G. *J. Am. Chem. Soc.* **1973**, *95*, 2477−2482. (b) Bailes, R. H.; Calvin, M. *J. Am. Chem. Soc.* **1947**, *69*, 1886−1893. (c) Weber, J. H.; Busch, D. H. *Inorg. Chem.* **1965**, *95*, 469−471. (d) Yang, Y.-C.; Ward, J. R.; Seiders, R. P. *Inorg. Chem.* **1985**, *24*, 1765−1769. (e) Boyce, S. D.; Hoffmann, M. R.; Hong, P. A.; Moberly, L. M. *Environ. Sci. Technol.* **1983**, *17*, 602−611. (f) In this approximation, the second fast electron transfer following the rds is accounted for by doubling the actual concentration of substrate in an EC_{cat} simulation, see Andrieux, C. P.; Blocman, C.; Dumas-Bouchiat, J.-M.; M'Halla, F.; Saveant, J.-M. *J. Electroanal. Chem.* **1980**, *113*, 19−40. (g) Nicholson, R. S.; Shain, I. *Anal. Chem.* **1964**, *36*, 706−723. (h) Maiya, G. B.; Han, B. C.; Kadish, K. M. *Langmuir* **1989**, *5*, 645−650. (i) This approach minimizes errors arising from the different types of baselines in the more often used ratio of anodic and cathodic peaks. (j) Rudolph, M; Reddy, D. P.; Feldberg, S. W. *Anal. Chem.* **1994**, *66*, 589A−600A.

(20) (a) Bard, A. J.; Faulkner, L. R. *Electrochemical Methods;* Wiley: New York, 1980. (b) Nicholson, R. S. *Anal. Chem.* **1965**, *37*, 1351−1355.

(21) (a) Chen, S. J.; Evans, D. F.; Ninham, B. W. *J. Phys. Chem.* **1984**, *88*, 1631−1634. (b) Zemb, T. N.; Hyde, S. T.; Derian, P.-J.; Barnes, I. S. Ninham, B. W. *J. Phys. Chem.* **1987**, *91*, 3814−3820.

(22) (a) Bruno, T. J.; Svoronos, P. N. D. *CRC Handbook of Basic Tables for Chemical Analysis;* CRC Press: Boca Raton, FL, 1989; p 89. (b) Fendler, J. H.; Nome, F.; Van Woert, H. C. *J. Am. Chem. Soc.* **1974**, *96*, 6745−6753.

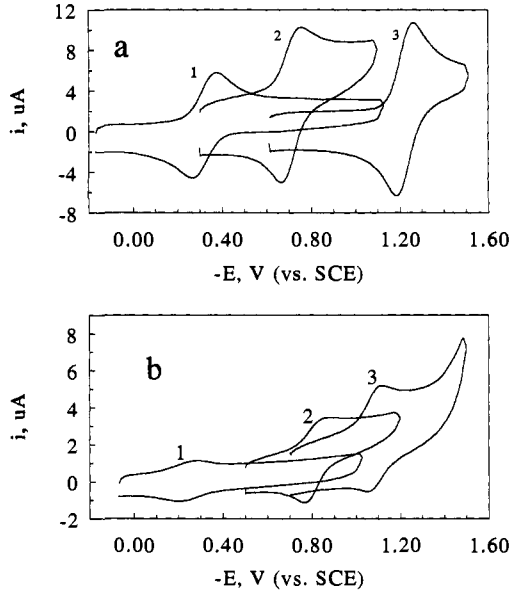

Figure 1. Cyclic voltammograms at 0.1 V s^{-1} on glassy carbon electrodes: (a) in 0.1 M TBABr/DMF for 6 × 10^{-4} M CoTSPc (**1**), vitamin B_{12r} (**2**), and Co(salen) (**3**); (b) in DDAB microemulsion for 3 × 10^{-4} M CoTSPc (**1**) and 4 × 10^{-4} M vitamin B_{12r} (**2**) and Co(salen) (**3**).

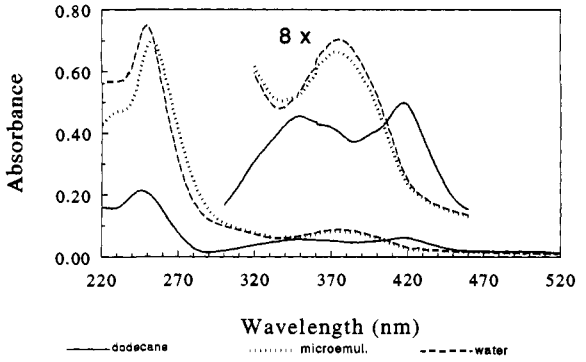

Figure 2. UV−vis spectra of Co(salen) in dodecane (saturated, *ca.* 5 μM), DDAB microemulsion (12 μM) and water (12.8 μM). Inset has 8-fold enhanced absorbance.

voltammetry of Co(salen) at frequencies above 30 Hz was obtained to estimate a formal potential in 0.1 M aqueous KBr similar to that in DMF. For vitamin B12r, a shift to more negative potentials was observed in the microemulsion compared to DMF, and the formal potential in water depends upon pH (Table 1).[7]

Residences Sites of Reactants. Previous phase distribution studies suggested that 1,2-dibromocyclohexane and other nonpolar organohalides reside almost entirely in the oil phase of microemulsions.[7] The highly water soluble vitamin B_{12} resides almost entirely in the water phase,[7,22b] as should the ionic cobalt phthalocyaninetetrasulfonate.

The electronic absorption spectrum of Co(salen) was similar in the microemulsion and in water with two bands at about 250 and 375 nm (Figure 2). Spectra in dodecane (Figure 2) are strikingly different, with bands at 247, 350, and 418 nm. These results confirm that Co(salen) resides predominantly in the water phase of the microemulsion.

Absorption spectroscopy was also used to estimate solubilities of Co(salen) in water and dodecane, from which a water/oil partition coefficient of >100 was predicted.

Reactions with *trans*-1,2-Dibromocyclohexane (DBCH). Reactions of Co(I) macrocycles with alkyl vicinal dibromides

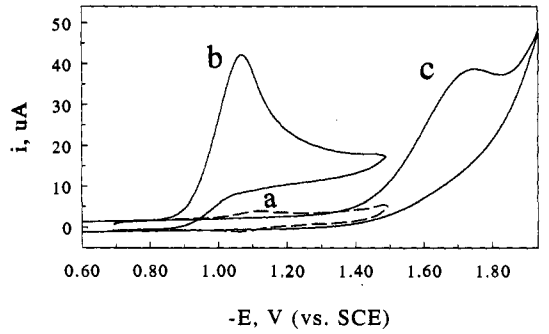

Figure 3. Cyclic voltammograms at 0.1 V s^{-1} on glassy carbon electrodes in the DDAB microemulsion: (a) 4 × 10^{-4} M Co(salen) alone; (b) 4 × 10^{-4} M Co^{II}(salen) + 1.5 × 10^{-3} M DBCH; and (c) 1.5 × 10^{-3} M DBCH alone without catalyst.

Scheme 1

$$Co(II)L + e^- \rightleftharpoons Co(I)L \qquad k^o' \quad \text{(at electrode)} \qquad (1)$$

$$Co(I)L + RBr_2 \rightarrow RBr^\bullet + Co(II)L + Br^- \quad (k_1, \text{rds}) \qquad (2)$$

$$Co(I)L + RBr^\bullet \rightarrow Co(II)L + Br^- + \text{olefin} \qquad (3)$$

or eq (1) followed by

$$Co(I)L + RBr_2 \rightarrow \text{olefin} + Br^- + Co(III)LBr \quad (k_1, \text{rds}) \qquad (4)$$

provide examples of fast inner sphere electron transfer reactions.[18,23] Cathodic currents greatly in excess of those for the Co(II) reduction peak of the catalyst alone were observed in solutions containing a cobalt complex and DBCH (Figure 3), and the peak is shifted slightly positive. No reverse peaks for oxidation of Co(I) were found except at scan rates above 10 V s^{-1}, suggesting a fast reaction of the Co(I) species with DBCH.

Upon decreasing concentration of DBCH, the cathodic current decreases. When concentration of DBCH is small enough or scan rate is large enough, anodic/cathodic peaks characteristic of the quasireversible Co(II)/Co(I) couple were again observed. In addition, the direct reduction peak of DBCH at the electrode occurs at potentials of about −1.75 V (Figure 3), much more negative than the Co(II)/Co(I) formal potential. These observations are consistent with the rapid catalytic reduction of DBCH by the cobalt complexes, as previously investigated in organic solvents[7,23] and in a water-in-oil microemulsion.[7]

The pathway in Scheme I, proposed for the catalytic reduction of alkyl vicinal dibromides in organic solvents and water-in-oil microemulsions[7,18,23] was tested for the present data. In Scheme I, the macrocyclic Co(I)L species formed at the electrode (eq 1) reacts with DBCH (RBr_2) in the rate determining step (rds, eq 2 or 4). Equation 2 yields radical $RBr^\bullet$ and Co(II)L. Radical $RBr^\bullet$ can be reduced by Co(I)L in a solution electron transfer (SET, eq 3), which is energetically favored compared to reduction at the electrode.[18] An alternative pathway involves eq 1 followed by the concerted E2 elimination in eq 4. This step is followed by reduction of Co(III)LBr to Co(I)L to complete the catalytic cycle. Equation 4 was proposed as the rds for reactions of vicinal dibromides with Fe(I) and Co(I) porphyrins based on steric hindrance studies.[23b] Both possible rate determining steps feature the bimolecular reaction of Co(I)L with RBr_2.[24]

The increased peak current for Co(II) reduction in solutions containing DBCH is called the catalytic current (i_c). Its variation

(23) (a) Lexa, D.; Saveant, J.-M., Su, K. B.; Wang, D. L. *J. Am. Chem. Soc.* **1987**, *109*, 6464−6470. (b) Lexa, D.; Saveant, J.-M.; Schafer, H. J.; Su, K.-B.; Vering, B.; Wang, D. L. *J. Am. Chem. Soc.* **1990**, *112*, 6162−6177.

(24) The bimolecular rate determining steps are kinetically indistinguishable, and data analysis procedures for obtaining k_1 are identical for these two mechanistic possibilites.

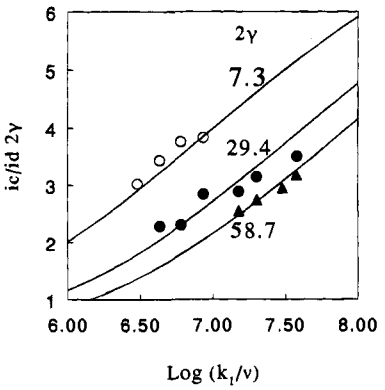

Figure 4. Catalytic efficiencies as $i_c/i_d2\gamma$ vs log (k_1/ν) in the DDAB microemulsion plotted for the av $k_1 = 3 \times 10^6\ M^{-1}\ s^{-1}$ for 4×10^{-4} M Co(salen) at three concentration ratios γ = [DBCH]/[Co(salen)]. Lines represent theoretical predictions from the simulations of Scheme 1. Points are experimental data.

with the concentration ratio of DBCH to catalyst (γ = [DBCH]/[catalyst]) and scan rate (ν) can be used to estimate the rate constant of the rate-determining step of the overall reaction.[18,23,25]

Values of k_1 were obtained with the aid of digital simulations (see Experimental Section), providing the simultaneous opportunity of testing Scheme I. Simulations of CVs using the values of D, $k^{o\prime}$, and $E^{o\prime}$ in Table 1, and D values for DBCH obtained from direct electrochemical measurements were used to construct theoretical curves of $(i_c/2\gamma i_d)$ vs log k_1/ν, where i_d is the diffusion current for catalyst in the absence of DBCH. Families of theoretical curves result, one for each value of γ (Figure 4). Rate constants were found by comparing experimental $i_c/2\gamma i_d$ values with the appropriate theoretical curve.

For a given cobalt complex, k_1 was constant over a wide range of scan rates and γ-values, as reflected by standard deviations (Table 2) on the order of ±10%. Goodness of fit of Scheme 1 to the data is illustrated by agreement of experimental points plotted using the average k_1 value for a particular reaction with the theoretical lines for each γ at a series of scan rates (Figure 4). Good agreement with theory for Scheme 1 was found in both media for all complexes with diffusion controlled Co(II)/Co(I) reactions.

Reactions with *n*-Alkyl Bromides. Alkylations of Co(I) complexes with alkyl halides can be initiated by generating the Co(I) reagent at an electrode.[26,27] With 1-bromoalkanes, the reaction is a second-order nucleophilic substitution (S_N2).[27-30]

Addition of *n*-butyl bromide or *n*-dodecyl bromide to DMF containing one of the cobalt complexes resulted in a partial or full disappearance of the anodic peak for oxidation of the Co(I)L complex at low scan rates (Figure 5), while the cathodic peak for Co(II)L reduction remained the same height. Similar results were obtained in the microemulsion (Figure 6). Complete disappearance of the anodic peak was facilitated by high concentrations of alkyl bromide and low scan rates. These results indicate[20a] that Co(I)L reacts with the alkyl bromide (RBr, Scheme 2) in a noncatalytic process.

A new peak appeared in the range −1.35 to −1.75 V vs SCE in solutions containing Co(II)L and alkyl bromide (Figures 5 and 6). Direct reduction of the alkyl bromides was not observable in either DMF or microemulsion. Thus, this new peak is attributed to the reduction of the product formed at the formal potential of Co(II)/Co(I) (eq 6)[13,31,32] and confirms formation of an alkyl−cobalt derivative. The voltammetric behavior is consistent with Scheme 2.

The second-order rate constant k_1 for the S_N2 alkylation (eq 6) was obtained from the ratio of anodic peak currents in the absence (i_{pa}^o) and the presence of the alkyl bromide (i_{pa}) at a series of scan rates and at a series of concentrations of butyl bromide and dodecyl bromide. These measurements were made on CVs with a switching potential negative of the Co(II) reduction peak but positive of the second reduction peak. As the concentration of organic halide was increased (Figures 5 and 6) or as scan rate was decreased, i_{pa}/i_{pa}^o decreased because of the influence of the second order chemical reaction on i_{pa}.

Digital simulations based on eqs 5 and 6 were used to construct theoretical curves of i_{pa}/i_{pa}^o vs log $k_1\tau$, where τ is the time between $E_{1/2}$ and the switching potential of the CV.[19g,20a] A different theoretical curve results from each concentration ratio γ = [RBr]/[Co(II)L] (Figure 7). Rate constants were estimated by comparisons of experimental i_{pa}/i_{pa}^o values with the appropriate theoretical curve.

Estimated rate constants for a range of γ and scan rates centered around a mean, with standard deviations within ±10% in most cases (Table 3). Good agreement of experimental and simulated data were obtained in all cases, as illustrated for a reaction in the microemulsion (Figure 7).

Discussion

Reduction of DBCH. Data for reactions of Co(I) complexes with DBCH in DMF and the bicontinuous microemulsion were consistent with Scheme 1. In a previous study in which vitamin B_{12} resided in water pools in AOT/water/isooctane water-in-oil (w/o) microemulsions and DBCH resided largely in the continuous oil phase, reaction rates (Table 2) were several orders of magnitude smaller[7] relative to homogeneous buffered pH 2.3 acetonitrile/water. Conversely, rate constants in the bicontinuous microemulsion are comparable in order of magnitude to those in DMF and much larger than in the w/o microemulsion.

Residences of catalysts in the water phase and DBCH in the oil are the same in the bicontinuous and w/o microemulsions, but the bicontinuous fluid provides much higher reaction rates. A possible explanation for faster kinetics in the bicontinuous fluid involves more effective phase mixing. Estimates based upon the radius of water droplets containing vitamin B_{12} in the w/o microemulsion and the length and diameter of the water conduits in the bicontinuous fluid show that the bicontinuous DDAB microemulsion has an interfacial surface area fourfold larger than the AOT w/o system.[33a] This may facilitate more intimate mixing of the reactants in the two different phases in the DDAB microemulsion. Faster interfacial dynamics may also play a role in increasing the mixing efficiency between reactants in the oil and water phases, although little information on this point is currently available. An increase in interfacial fluidity caused by addition of cosurfactant was recently suggested as

(25) (a) Andrieux, C. P.; Blocman, C.; Dumas-Bouchiat, J.-M.; Saveant, J.-M. *J. Am. Chem. Soc.* **1979**, *101*, 3431−3441. (b) Andrieux, C. P.; Hapiot, P.; Saveant, J.-M. *Chem. Rev.* **1990**, *90*, 723−738. (c) Because adsorption of CoTSPc onto the electrode in the microemulsion violated the criterion of homogeneous reactions, rates for this reaction were only measured in DMF.

(26) (a) Costa, G.; Puxeddu, A.; Reisenhofer, E. *J. Chem. Soc. (Dalton)*, **1973**, 2034−2039. (b) Lexa, D.; Savéant, J.-M.; Soufflet, J. P. *J. Electroanal. Chem.* **1979**, *100*, 159−172.

(27) (a) Lexa, D.; Mispelter, J.; Saveant, J.-M. *J. Am. Chem. Soc.* **1981**, *103*, 6806−6812. (b) Zhou, D.-L.; Walder, P.; Scheffold, R.; Walder, L. *Helv. Chim. Acta* **1992**, *75*, 995−1011.

(28) Saveant, J.-M. *Adv. Phys. Org. Chem.* **1990**, *26*, 1−130.

(29) Schrauzer, G. N.; Deutsch, E. *J. Am. Chem. Soc.* **1969**, *91*, 3341−3350.

(30) (a) *B_{12}, Vol. I;* Dolphin, D., Ed.; Wiley: New York, 1982. (b) Toscano, P. J.; Marzilli, L. G. *Prog. Inorg. Chem.* **1984**, *31*, 105−204.

(31) Lexa, D.; Saveant, J.-M. *J. Am. Chem. Soc.* **1978**, *100*, 3220−3222.

(32) Zhou, D.-L.; Tinembart, O.; Scheffold, R.; Walder, L. *Helv. Chim. Acta* **1990**, *73*, 2225−2241 and references therein.

Table 2. Rate Constants for Reduction of DBCH by Cobalt(I) Complexes[a]

reactant[b]	medium	N[c]	k_1 (mean ± SD),[d] M^{-1} s^{-1}	$-E_{1/2}$,[e] V vs SCE	ΔE,[f] V
Co^{I}TSPc	DMF	26	8.85 ± 0.77	0.312	1.316
Co^{I}(salen)	DMF	14	(4.31 ± 0.54) × 10^6	1.122	0.415
	bicontinuous microemulsion	28	(3.02 ± 0.30) × 10^6	0.985	0.490
vit. B_{12s}	DMF	35	(5.58 ± 0.95) × 10^4	0.688	0.930
	bicontinuous microemulsion	22	(2.42 ± 0.26) × 10^5	0.786	0.760
	0.2 M AOT(w/o)[g]		6 × 10^3	0.847	see ref 7

[a] DBCH: Abbreviation of (±)-*trans*-1,2-dibromocyclohexane. [b] For simplicity, the overall charge of the catalyst has been omitted. [c] Number of trials. [d] Mean value of k_1 obtained from CVs with different γ = [DBCH]/[catalyst] at different scan rates; see text. [e] Value taken from catalytic wave at low γ. [f] $\Delta E = E^{o\prime}(Co^{II}L/Co^{I}L) - E_{1/2}$ (DBCH). [g] 0.2 M AOT/4 M H_2O/isooctane; from ref 7.

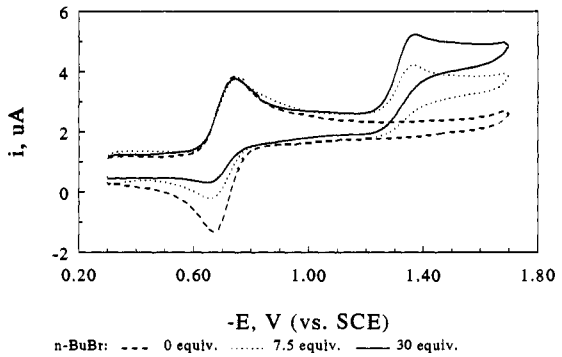

Figure 5. Cyclic voltammograms at 0.02 V s^{-1} on glassy carbon electrodes for 6 × 10^{-4} M vitamin B_{12r} in 0.1 M TBABr/DMF with various equivalent ratios (γ) of *n*-butyl bromide.

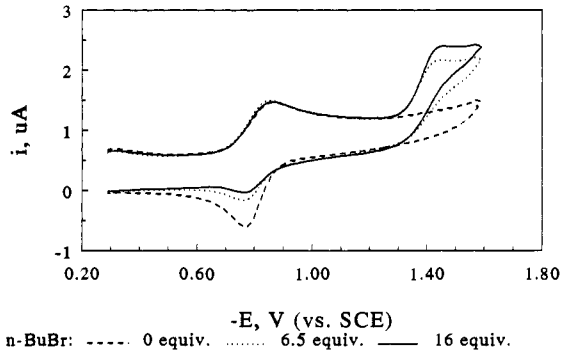

Figure 6. Cyclic voltammograms at 0.02 V s^{-1} on glassy carbon electrodes for 7 × 10^{-4} M vitamin B_{12r} in DDAB microemulsion with various equivalent ratios (γ) of *n*-butyl bromide.

Scheme 2

$Co(II)L + e^- \rightleftharpoons Co(I)L$ $k^{o\prime}$, at $E^{o\prime}_1$ (at electrode) (5)

$Co(I)L + RBr \rightarrow R\text{-}Co(III)L + Br^-$ (k_1) (6)

$R\text{-}Co(III)L + e^- \rightarrow Co(I)L + R^\bullet$ at $E^{o\prime}_2 << E^{o\prime}_1$ (at electrode) (7)

the cause for facilitated electron transfer at electrodes in AOT microemulsions.[33b]

A plot of log k_1 vs $E^{o\prime}_{Co(II)/Co(I)}$ for all the data is approximately linear (Figure 8). Rate constants in the bicontinuous microemulsion and in DMF fall on the same line with those for

(33) (a) For the AOT w/o system,[7] the hydrodynamic radius of water droplets containing vitamin B_{12} was 75 Å. A head group area of 60 Å gives about 1200 molecules of AOT per droplet and a total interfacial surface area of 7 × 10^{21} $Å^2$ per mL. For the DDAB microemulsion used in this work, a water conduit length of 3.5 × 10^{20} Å per mL and a radius of 13.2 Å was estimated.[11c] Treating the conduits as a single cylinder with these dimensions gives an estimated interfacial surface area of 3 × 10^{22} $Å^2$ per mL. Based on these estimates, the interfacial surface area of the DDAB microemulsion is 4.3-fold larger than that of the AOT w/o microemulsion. (b) Garcia, E.; Song, S.; Oppenheimer, L. E.; Antalek, B.; Williams, A. J.; Texter, J. *Langmuir* **1993**, *9*, 2782–2785.

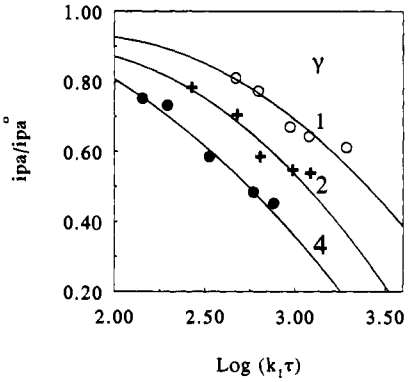

Figure 7. Ratio of anodic peak currents in absence ($i_{pa}°$) and presence (i_{pa}) of *n*-butyl bromide vs log ($k_1\tau$) in the DDAB microemulsion plotted for the av k_1 = 354 M^{-1} s^{-1} for 4 × 10^{-4} M Co(salen) at three concentration ratios γ = [RBr]/[Co(salen)]. Lines represent theoretical predictions from the simulations of Scheme 2. Points are experimental data.

Table 3. Rate Constants for Alkylation of Cobalt(I) Complex by Alkyl Bromides[a]

cobalt(I) complex[b]	medium[c]	*n*-RBr	N[d]	$10^{-2}k_1$ (mean ± SD),[e] M^{-1} s^{-1}	$-E_{pc}$,[f] V vs SCE	ΔE,[g] V
Co^{I}(salen)	DMF	*n*-BuBr	26	21.0 ± 1.1	1.731	0.506
		n-$C_{12}H_{25}$Br	15	79.1 ± 4.7	1.736	0.511
	DDABμE	*n*-BuBr	31	3.54 ± 0.21	1.511[h]	0.426
		n-$C_{12}H_{25}$Br	29	6.21 ± 0.67	1.504[h]	0.419
vit. B_{12s}	DMF	*n*-BuBr	17	0.066 ± 0.005	1.376	0.666
		n-$C_{12}H_{25}$Br	7	0.165 ± 0.009	1.381	0.671
	DDABμE	*n*-BuBr	9	0.075 ± 0.012	1.432[h]	0.617
		n-$C_{12}H_{25}$Br	12	0.267 ± 0.052	1.399[h]	0.584

[a] See Experimental Section for exact conditions. [b] For simplicity, the overall charge of the catalyst has been omitted. [c] 0.1 M TBABr/DMF; μE = microemulsion. [d] Number of trials. [e] Mean value of k_1 obtained from the CVs with different [*n*-RBr]/[Co(II)L] at series of scan rates. [f] Value taken from the second wave attributed to the reduction of the *in-situ* generated R-Co^{III}L. [g] $\Delta E = E^{o\prime}(Co^{II}L/Co^{I}L) - E_{pc}$(R-$Co^{III}$L). [h] Estimated E_{pc} value from LSV at low substrate concentration.

reduction of DBCH by other inner sphere cobalt complexes in DMF.[23] Thus, the main reason for differences in rates of catalytic DBCH reduction is the differences in formal potentials of the Co(II)/Co(I) couples. There appears to be little influence of kinetic control by distribution of reactants in the two phases, which was the major reason for smaller rate constants in the w/o microemulsion.[7]

Rate constants for reduction of DBCH by the cobalt complexes are consistent with inner sphere electron transfer. When rate constants for known outer sphere reactants are included in the log k_1 vs $E^{o\prime}$ plots, it can be seen that rates for reactions of DBCH with Co^{I}(salen) and vitamin B_{12s} are much larger compared to an outer sphere reactant with the same $E^{o\prime}$ (Figure 8). This is because of the lower activation energy of the inner

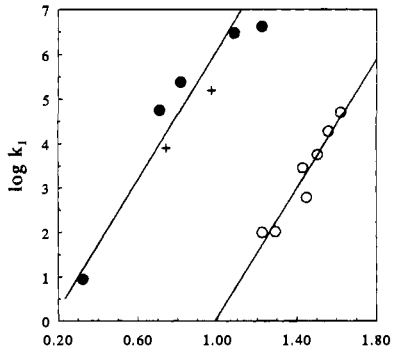

Figure 8. Influence of the Co(II)/Co(I) formal potential on log k_1 for reactions of Co(I) complexes with DBCH in DMF and in the DDAB microemulsion. Results at 25 °C from Table 2 (•); rate constants in DMF at 21 ± 1 °C for inner sphere catalysts (+) cobalt octaethylporphyrin (−0.97 V, ref 23a) and cobalt tetraphenylporphyrin (−0.75 V, ref 23b); rate constants in DMF at 21 °C for outer sphere electron transfer catalysts (o) perylene (−1.62 V), zinc octaethylporphyrin (−1.56 V), terephthalonitrile (−1.50 V), benzo[*c*]chinoline (−1.45 V), copper octaethylporphyrin (−1.43 V), octaethylporphyrin (−1.29 V), and 9-fluorenone (−1.23 V) (data from ref 23).

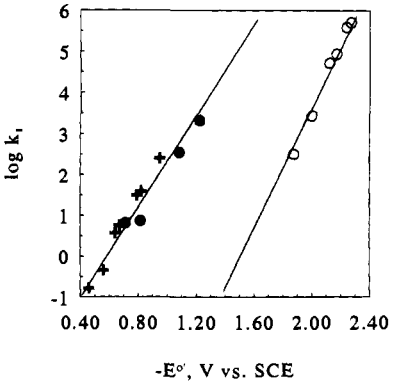

Figure 9. Influence of the Co(II)/Co(I) formal potential on log k_1 (Table 3) for the S_N2 reaction of Co(I) complexes with *n*-butyl bromide in DMF and DDAB microemulsion at 25 °C (•). Rate constants for the S_N2 reaction of Co(I) porphyrins with *n*-butyl bromide in DMF at 25 °C (+); cobalt octaethylporphyrin (−0.95 V), cobalt 5,10,15,20-tetrakis-(*p*-methoxyphenyl)porphyrin (−0.82 V); cobalt tetraphenylporphyrin (−0.79 V), cobalt 5,10,15,20-tetrakis(*p*-trifluorophenyl)porphyrin (−0.67 V), cobalt 5,10,15,20-tetrakis(4-trimethylammoniumphenyl)porphyrin (−0.64 V), cobalt 5,10,15,20-tetrakis(pentafluorophenyl)porphyrin (−0.56 V), cobalt 5,10,15,20-tetrakis(1-methylpyridinium-4-yl)porphyrin (−0.46 V) (data from ref 36a). Rate constants in DMF at 20 °C of outer sphere electron transfer reactions of *n*-butyl bromide (o) with anion radicals of *m*-toluonitrile (−2.27 V), benzonitrile (−2.24 V), methyl benzoate (−2.17 V), benzo[*h*]chinoline (−2.12 V), phenanthridine (−2.00 V), and anthracene (−1.875 V) (data from ref 36b).

sphere pathway,[28] leading to a *kinetic advantage* compared to outer sphere electron transfer.

Reactions with *n*-Bromoalkanes. Data for reactions with the Co(I) complexes in both media were consistent with the mechanism in Scheme 2, eqs 5 and 6. The second peak at potentials more negative than $E^{\circ\prime}_{Co(II)/Co(I)}$ confirms the formation of the alkyl−cobalt products (eq 7). Although the two reactants are in different phases, rate constants in the microemulsion differ by less than one order of magnitude from those in DMF.

An S_N2 reaction such as that between Co(I) complexes and *n*-alkyl bromides may be viewed as an inner sphere electron transfer. This is justified in the sense that bond breaking and formation are concerted with transfer of a single electron.[27,28] An equivalent concept is that of a "single electron shift" from the nucleophile to the halide.[34,35] In this context, the nucleophile can be considered an electron donor.[28] Consequently, rate constants of S_N2 reactions of a series of nucleophile−electrophile pairs should depend on the difference in formal potentials of the two reactants, provided differences in steric interactions in the transition state are negligible. For a given alkyl halide, k_1 should depend logarithmically on the formal potential of the M(II)/M(I) redox couple. Such a relationship has been observed previously for reactions of alkyl halides with iron porphyrins[27a,28] and cobalt porphyrins.[36a]

In agreement with the above concept, a plot of log k_1 vs $E^{\circ\prime}_{Co(II)/Co(I)}$ for *n*-butyl bromide shows excellent linearity (Figure 9). Rate constants for the microemulsion and DMF fall on the same line as data obtained previously for the alkylation of Co(I) porphyrins with *n*-butyl bromide in DMF.[36a] A similar plot was obtained for *n*-dodecyl bromide (Figure 10). As for the catalytic reduction of DBCH, rates of the S_N2 reactions are correlated with formal potentials of the cobalt complexes.

The kinetic advantage of the S_N2 reaction viewed as an inner sphere electron transfer can be seen by comparing rate constants with those for reactions of *n*-butyl bromide with a series of outer sphere electron transfer agents[36b] (Figure 9, open circles). Rates for the S_N2 reaction of *n*-butyl bromide are significantly larger

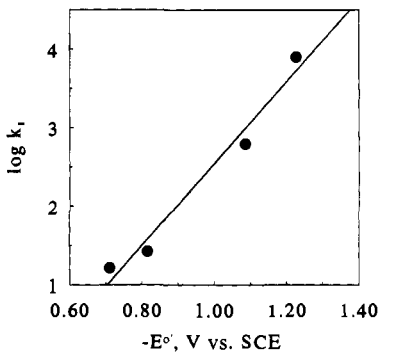

Figure 10. Influence of the Co(II)/Co(I) formal potential on log k_1 (Table 3) for the S_N2 reactions of Co(I) complexes with *n*-dodecyl bromide in DMF and the DDAB microemulsion.

Scheme 3

$$\begin{array}{ccc} Co(II)L_S + e^- & \rightleftharpoons & Co(I)L_S \\ \Updownarrow (K_O) & & \Updownarrow (K_R) \\ Co(II)L_W + S + e^- & \rightleftharpoons & Co(I)L_W + S \end{array}$$

than those of outer sphere electron transfers for reactants with the same $E^{\circ\prime}$.

Factors Controlling $E^{\circ\prime}$. The most likely influences on Co(II)/Co(I) formal potentials are solvent and pH effects and specific interactions with surfactant. Concerning the latter, a model for interactions of electroactive reactants with surfactant micelles,[3] recently extended to microemulsions,[37] may be invoked (Scheme 3).

Here, $Co(II)L_S$ and $Co(I)L_S$ represent complexes bound to the surfactant monolayer (S) separating the oil and water phases. The water phase contains the unbound complexes $Co(II)L_w$ and $Co(I)L_w$. Partition coefficients K_O and K_R between water and interfacial surfactant layers are

(34) Pross, A.; Shaik, S. S. *Acc. Chem. Res.* **1983**, *16*, 363−370.
(35) Pross, A. *Acc. Chem. Res.* **1985**, *18*, 212−219.
(36) (a) Yang, D. H.; Zhou, D.-L.; Walder, L., unpublished results. (b) Andrieux, C. P.; Gallardo, I.; Saveant, J.-M.; Su, K.-B. *J. Am. Chem. Soc.* **1986**, *108*, 638−647.
(37) Myers, S. A.; Mackay, R. A.; Brajter-Toth, A. *Anal. Chem.* **1993**, *65*, 3447−3453.

$$K_O = [Co(II)L_w]/[Co(II)L_S] \quad \text{and} \quad K_R = [Co(I)L_w]/[Co(I)L_S] \quad (8)$$

The reversible half-wave (formal) potential in the microemulsion ($E_{1/2,r}$) is given by[3,37]

$$E_{1/2,r} = E^{\circ\prime}_w + (RT/F)\ln\{K_O(1 + K_R)/K_R(1 + K_O)\} - (RT/2F)\ln[D_O/D_R] \quad (9)$$

where $E^{\circ\prime}_w$ is the formal potential in water, and D_O and D_R are measured diffusion coefficients for oxidized and reduced forms of the complex in the microemulsion.

Co^{II}(salen) has zero charge and resides predominantly in the water phase. Its reduction product, $[Co^{I}(salen)]^-$, is negatively charged and can interact with the positively charged headgroups of the surfactant. In this situation, we can assume $K_O > 1 > K_R$. To a first approximation eq 9 becomes

$$E_{1/2,r} = E^{\circ\prime}_w + (RT/F)\ln(1/K_R) - (RT/2F)\ln[D_O/D_R] \quad (10)$$

Since, $K_R < 1$, $E_{1/2,r}$ should be more positive than $E^{\circ\prime}_w$. This is the case for Co(salen) (Table 1). Approximating D_R by the self-diffusion coefficient of DDA^+ in the microemulsion, found by NMR[9b] to be 3×10^{-7} cm^2 s^{-1}, and taking D_O from Table 1, the last term in eq 10 equals -8 mV. Using values of $E_{1/2,r}$ and $E^{\circ\prime}_w$ from Table 1 with eq 10 gives an estimate of 8×10^{-4} for K_R.

Thus, the difference of 140 mV in formal potentials of Co(salen) in the microemulsion and DMF can be attributed mainly to the interaction of the $[Co^{I}(salen)]^-$ with surfactant. The similarities of $E^{\circ\prime}$ of Co(salen) in water and DMF suggest that specific solvation does not make a large contribution to differences in formal potentials.

Shifts in $E^{\circ\prime}$ with pH for vitamin B_{12} Co(II)/Co(I) (cf. Table 1) result mainly from protonation of the benzimidazole side chain attached to the B_{12} corrin ring.[38] When unprotonated, this benzimidazole becomes an axial ligand on cobalt. We recently used a kinetic method involving protonation of a radical to estimate[39] a water phase pH of 4.7 in the DDAB microemulsion used in the present study.[40] The $E^{\circ\prime}$ of -0.815 V for B_{12}Co(II)/Co(I) in the microemulsion is similar to that of -0.83 V at pH 4.7 in aqueous buffer.[38] Furthermore, studies of electronic spectra suggested little specific interaction of vitamin B_{12} with cationic surfactant head groups in aqueous micelles and microemulsions.[22b] We conclude that the major determinant of formal potential for vitamin B_{12} in the microemulsion is the pH of the water phase.

Studies of the pH dependence of the electrochemistry of vitamin B_{12} have shown that between pH 3 and 4.7, the electrode reaction and $E^{\circ\prime}$ range in water are[38]

$$H^+ + [Co(II)L'] + e^- \rightleftharpoons [Co(I)]\sim L'H^+ \quad -0.74\ V < E^{\circ\prime} < -0.85\ V \quad (11)$$

while at pH>4.7

$$[Co(II)L'] + e^- \rightleftharpoons [Co(I)]\sim L' \quad E^{\circ\prime} = -0.85\ V \text{ (all vs SCE)} \quad (12)$$

where L′ represents the benzimidazole side chain, acting as an axial ligand when it is inside the square parentheses. Considering the estimated pH of the water phase and the $E^{\circ\prime}$ value found for B_{12}Co(II)/Co(I), eq 11 seems likely to be the primary contributor to voltammetry in the microemulsion, with a minor role for eq 12.

Overall, [Co(II)L′] is uncharged. After accepting an electron and a proton (eq 11), its reduction product $[Co(I)]\sim L'H^+$ remains uncharged. Neither of these species would interact strongly with surfactant head groups, consistent with the view that pH is the main determinant of $E^{\circ\prime}$ for B_{12}Co(II)/Co(I) in the microemulsion.

Conclusions

This work demonstrates that rates of electrochemically initiated bimolecular reactions in bicontinuous microemulsions can be as fast as in homogeneous solvents, even when the two reactants reside in different phases and the reaction does not occur on the electrode surface. Results demonstrate a kinetic advantage of bicontinuous over w/o microemulsions, possibly because of more efficient reactant mixing in the bicontinuous system which has a larger interfacial area. The bicontinuous DDAB microemulsion resembles a homogeneous solvent containing a proton donor (see eq 11). This is in agreement with previous studies on the electrochemical reduction of polyaromatic hydrocarbons in the same DDAB microemulsion.[10,11]

For a given alkyl bromide, activation free energies governing rate constants of catalytic and S_N2 reactions were controlled mainly by the formal potential of the Co(II)/Co(I) redox couple, which was influenced by specific interactions in the microemulsion. Control of formal potentials by microemulsion composition was demonstrated recently.[37,41] Thus, it may be possible to control rates of bimolecular reactions in bicontinuous microemulsions by controlling the formal potentials of reactants with the appropriate system composition.

Acknowledgment. This work was supported mainly by a grant from NSF (CTS-9306961) and partly by a grant from the CT Department of Economic Development. The authors thank L. Walder of Ecole Polytechnique Lausanne for permission to use unpublished data for S_N2 reactions of cobalt porphyrins in DMF in Figure 9. They also thank Al Fry of Wesleyan University for helpful discussions and Qingdong Huang for help with analyzing data.

JA9432776

(38) Lexa, D.; Saveant, J.-M. *Acc. Chem. Res.* **1983**, *16*, 235–243.
(39) Gounili, G.; Miaw, C. L.; Bobbitt, J. M.; Rusling, J. F. *J. Colloid Interface Sci.*, **1992**, *153*, 446–456.
(40) A weakly acidic water phase results from attraction of hydroxide ions to head groups at the oil–water interface. This leaves excess hydronium ions in the water phase.[39]
(41) Mackay, R. A.; Myers, S. A.; Bodalbhai, L.; Brajter-Toth, A. *Anal. Chem.* **1990**, *62*, 1084–1090.